INTERFACIAL INTERACTIONS AND REINFORCEMENT IN THERMOPLASTICS/ZEOLITE COMPOSITES

Dóra Andrea Kajtár[1,2], Csaba Kenyó[1,2], Károly Renner[1,2,*], János Móczó[1,2], Erika Fekete[1,2], Christoph Kröhnke[3] and Béla Pukánszky[1,2]

[1]Laboratory of Plastics and Rubber Technology, Budapest University of Technology and Economics, H-1521 Budapest, P.O. Box 91, Hungary

[2]Institute of Materials and Environmental Chemistry, Research Centre for Natural Sciences, Hungarian Academy of Sciences, H-1519 Budapest, P.O. Box 286, Hungary

[3]Clariant Produkte (Deutschland) GmbH, D-81477 München, Germany

*Corresponding author: Phone: +36-1-463-2479, Fax: +36-1-463-3474, Email: krenner@mail.bme.hu

ABSTRACT

Ten different polymers were selected as possible matrices for zeolite containing desiccant composites in order to prepare functional packaging material. A 5A type zeolite was used as desiccant. Composites containing the zeolite up to 50 vol% were prepared. Interfacial adhesion was estimated by various means including the measurement of surface characteristics, cyclic loading experiments and evaluation of composition dependence of mechanical properties by appropriate models. The results showed that composite properties change in a wide range. The deformability of most composites is small and decreases with increasing zeolite content. Interfacial adhesion between the matrix polymer and the zeolite is not very strong, although quantitative determination is hampered by various factors. Most of the composites fail by debonding, brittle matrices

by debonding and/or matrix fracture, while considerable shear yielding has been observed in LDPE composites. Composite properties are determined mainly by matrix characteristics; interfacial adhesion plays only a relatively minor role.

1. INTRODUCTION

Structural materials are being replaced in increasing quantities by functional materials, which, besides their excellent mechanical properties, also fulfill some function thus increasing their value [1]. A wide range of functions can be introduced into these materials like electrical and thermal properties, piezoelectric response, desiccant characteristics, antiseptic properties, etc. Desiccant characteristic are used mainly in the packaging industry, the most frequently in electronics [2] and pharma [3-5]; they can be achieved by combining polymers with fillers which adsorb or absorb water. The simplest and industrially most viable solution is the use of a desiccant filler, usually a silica gel [6] or zeolite [7]. The fillers adsorb water on their large, high energy surface thus preventing the contact of the packaged ware with humidity. Occasionally the filler may fulfill more than one function as in the preparation of breathable films, in which they help the formation of voids to let vapor pass through the film, but prevent the permeation of liquids, while act as desiccant at the same time. Zeolites were used for this purpose in more than one case [8-12].

Obviously, the components of the material and the ensuing composite must meet some requirements in order to fulfill their functions. Desiccant characteristics require large specific surface area and high surface energy to bind efficiently as much water as possible. On the other hand, matrix-filler adhesion cannot be excessively strong, otherwise debonding does not occur during the preparation of breathable films, and the required voids do not form. All packaging materials must possess certain mechanical properties to fulfill their role, stiffness, strength, deformability and fracture resistance must exceed certain minimum values. The mechanical properties of all heterogeneous

materials are determined by four factors: component properties, composition, structure and interfacial interaction [13]. This latter characteristic plays an important role in the preparation of breathable films, but interactions influence desiccant properties as well.

Because of the importance of interactions and adhesion, several attempts have been made to determine or estimate them. Unfortunately, published information is controversial sometimes coming even from the same authors. Biswas et al. [8-11, 14, 15] prepared zeolite composites with various matrices including linear low density (LLDPE), low (LDPE) and high density (HDPE) polyethylene as well as polypropylene (PP). They drew their conclusions about adhesion from the composition dependence of tensile properties and from scanning electron micrographs (SEM). They claim strong interaction in LLDPE, but weak in the rest of the polyolefins. The conclusion is difficult to believe, since the surface energy of all polyolefins is small and very similar, interaction is created by van der Waals forces, thus it must be practically the same for all the polymers tested. Moreover, the authors neglected the fact that the composition dependence of mechanical properties is influenced also by matrix characteristics thus reinforcement is much stronger in a soft than in a hard matrix even at the same level of adhesion [16]. Similarly contradictory and confusing conclusions were published by other groups as well. Upadhyay et al. [17] claim strong adhesion between zeolite and polyamide (PA) based on the simple argument that both are polar. Similarly to Biswas et al. [14, 15], Balkose et al. [7, 12, 18] used the composition dependence of mechanical properties to estimate interactions in polypropylene/zeolite composites and found that they are weak. Other groups [19, 20] used SEM micrographs to evaluate interfacial adhesion and based on the fact that on fracture surfaces the filler is covered by the polymer they claim strong adhesion even when the surface of the zeolite was treated with aliphatic carboxylic acids [19] that are known to decrease surface energy and interactions [21].

The results are clearly contradictory and one of the reasons is that the composition dependence of tensile properties and SEM do not allow the reliable estimation of interfacial adhesion. In view of these contradictions the goal of our study was to estimate interfacial interactions and reinforcement in polymer zeolite composites potentially used

as desiccant packaging materials. The desiccant characteristics of the composites have been evaluated and reported in another paper [22]. In this communication we focus on interfacial interactions and try to point out the difficulties in their estimation, show the effect of matrix characteristics and discuss some practical consequences.

2. EXPERIMENTAL

2.1. Materials

Polymers with various chemical compositions, mechanical and rheological properties were selected for the study to cover a wide range of properties important in fulfilling their function in desiccant composites. A low (LDPE, Tipelin FA 24451, TVK, Hungary) and a high density (HDPE, Tipelin BA 55013, TVK, Hungary) polyethylene, a polypropylene (PP, Tipolen H 649 F, TVK, Hungary), a polystyrene homopolymer (PS, Sytron 686 E, Dow, USA), two high impact polystyrenes (HIPS1, Styron 485, HIPS2, Styron 1175, Dow, USA), a styrene-acrylonitrile copolymer (SAN, Tyril 880, Dow, USA), a polycarbonate (PC, Macrolon 2658, Bayer, Germany), a poly(methyl methacrylate) (PMMA, Ortoglas HFI 7, Arkema, France) and a PVC compound based on the Ongrovil S 5258 suspension grade powder of BorsodChem, Hungary were used as matrix polymers. Their most important characteristics are compiled in **Table 1**. A 5A type zeolite was selected as desiccant (Luoyang Jianlong Chem. Ind. Co., China). Its average particle size was 4.5 μm, density 1.66 g/cm^3 and specific surface area 533 g/m^2 as determined by nitrogen adsorption (BET). The theoretical pore diameter of this zeolite is 4.3 Å.

2.2. Sample preparation

Before composite preparation the zeolite was dried at 300 °C for 16 h in vacuum. The components were homogenized in a Brabender W 50 EH internal mixer attached to a Haake Rheocord EU 10 V driving unit at 190 °C for 10 min. PC was mixed with the zeolite at 240 °C. For further studies 1 mm thick plates were compression molded from the homogenized material at 190 or 240 °C using a Fontijne SRA 100 laboratory machine.

The zeolite content of the composites changed between 0 and 50 vol%.

2.3. Characterization

The molecular weight of the polymers was determined by gel permeation chromatography (Waters e2695 Separation Module) in THF or TCB, respectively, at 0.5 ml/min flow rate and 35 °C using a Water 2414 refractive index detector. The Styragel columns used were calibrated with polystyrene standards. Density was measured by using a pycnometer at room temperature. The zeolite content of the composites was checked by thermal gravimetry (TGA). 15 mg samples were heated to 650 °C at 80 °C/min rate in oxygen and kept there for 5 min to burn off the polymer.

The surface tension of the polymers was determined by static contact angle measurements. Normal alkanes were used for the determination of the dispersion component of surface tension, while six different solvents (water, glycerol, ethylene glycol, dimethyl sulfoxide, formamide, and 1-bromonaphthalene) were applied for the estimation of the polar component. The surface tension of the zeolite was determined by inverse gas chromatography (IGC). The filler was agglomerated with water and the 800-1200 µm fraction was used for the packing of the column. The dispersion component of surface tension was determined by the injection of n-alkanes at various temperatures between 200 and 280 °C. Unfortunately, none of the polar solvent eluted from the column thus the polar component of surface tension of the zeolite could not be determined with this method.

The mechanical properties of the composites were characterized by tensile testing using an Instron 5566 universal testing equipment at a gauge length of 115 mm. Cross-head speed was 0.5 mm/min during the determination of stiffness, while properties at larger deformations, i.e. yield stress and strain as well as tensile strength and elongation-at-break were determined at 5 mm/min. Debonding stress was estimated by cyclic loading experiments. The specimen was deformed up to different, increasing deformations at 0.5 mm/min cross-head speed. After reaching the desired deformation it was removed from the grips, was let to relax for 15 min and then deformed to the next, larger elongation.

Young's modulus was determined in each deformation step and debonding stress as well as the amount of debonded filler were derived from the deformation dependence of stiffness. The distribution of the zeolites in the composites and fracture mechanism were studied by scanning electron microscopy using a Jeol JSM 6380 LA apparatus. Micrographs were recorded on fracture surfaces created during tensile testing.

3. RESULTS AND DISCUSSION

The results are presented in several sections. First the composition dependence of properties are shown and then the reinforcing effect of zeolite in the various polymers is discussed next. Cyclic loading and the debonding of the desiccant is described in the following section, while issues related to interfacial adhesion are discussed in the last part of the paper.

3.1. Properties

As mentioned in the introductory part, besides desiccant characteristics, i.e. the capacity and rate of water adsorption [22], other properties are also important for the application of polymer/zeolite composites as packaging materials. Usually stiffness, strength and deformability are the mechanical properties to consider. The Young's modulus of selected composites is plotted against composition in **Fig. 1**. Only a few of the ten polymers is shown in the figure to facilitate viewing; the presentation of all results in a single figure results in a very confusing graph. The continuous lines are drawn only to guide the eye in this and in all other figures, they are not fitted correlations. Accordingly, the number of lines often do not correspond to the number of series in a given figure.

The stiffness prepared from the four polymers presented in **Fig. 1** covers a very wide range; it changes from about 0.3 up to around 10 GPa. The values for the composites produced with the other polymers are located between the two correlations bounded by LDPE and SAN. Stiffness increases with increasing zeolite content, as expected, the slope of the increase depends very much on the polymer used as matrix. As a consequence, a

product with practically any stiffness can be prepared from the polymers studied in this work, but of course functional characteristics as well as other mechanical properties must be also considered.

Composite strength is presented in **Fig. 2** for the same composites as in the previous figure. Composition dependence is different from that shown by stiffness, strength decreases in some matrices while increases in others. The decrease of strength is often interpreted as a sign of weak interaction between the matrix and the reinforcement, while the increase as strong interfacial adhesion. Such a simplistic explanation is completely misleading, composition dependence and the extent of reinforcement depends on the stiffness of the matrix as well. The filler or reinforcement carries much more load in a weak matrix than in a stiffer one [16]. Similarly to stiffness, strength values measured for the rest of the composites prepared with the remaining polymers as matrix are located within the boundaries set by LDPE and SAN.

The deformability of the composites characterized by their elongation-at-break is plotted as a function of composition in **Fig. 3** for the composites of the two previous figures. Elongation is plotted in a logarithmic scale because of the very large differences among the composites; ultimate deformation is almost 1000 % for LDPE, while only a few percent at most for stiffer composites. Only two lines are presented here, since the deformability of three of the composites is very similar to each other and very small. In fact most of the composites prepared from the other polymers not shown in the figure have very small deformability, thus one expects also their fracture resistance being quite small. If composites with considerable deformability and impact resistance must be prepared for a certain application, the choice is limited since the desiccant decreases the deformability of the matrix polymers very much.

3.2. Reinforcement

The strength and deformability of composites depends very much on the strength of interfacial interactions. Reinforcement cannot be judged by the mere observation of the composition dependence of stiffness, yield stress or strength. One must consider the fact that the polymer always wets the high energy surface of mineral fillers and a certain

interaction always develops between the components. Reinforcement, i.e. the load-bearing capacity of the second component, can be estimated quantitatively by the use of models; a model was developed earlier to describe the composition dependence of tensile yield stress [23], tensile strength [24] or fracture resistance [25] of particulate filled polymers. The model takes the following form for tensile strength

$$\sigma_T = \sigma_{T0} \, \lambda^n \, \frac{1-\varphi}{1+2.5\,\varphi} \exp(B\,\varphi)$$

(1)

where σ_T and σ_{T0} are the true tensile strength ($\sigma_T = \sigma\lambda$ and $\lambda = L/L_0$, where L is the ultimate and the L_0 initial gauge length of the specimen) of the composite and the matrix, respectively, n is a parameter taking into account strain hardening, φ is the volume fraction of the filler and B is related to its relative load-bearing capacity, i.e. to the extent of reinforcement, which, among other factors, depends also on interfacial interactions. If **Eq. 1** is transformed into a linear form and the natural logarithm of reduced tensile strength is plotted against filler content, a linear correlation is obtained, the slope of which is proportional to the load-bearing capacity of the reinforcement and under certain conditions to the strength of interaction. The tensile strength of two of the composite series is plotted in this way in **Fig. 4**. The correlations are linear indeed and their slope depends on the properties of the matrix, steep for the soft matrix (LDPE) and small for the stiff polymer (SAN). Accordingly, zeolite reinforces soft polymers much more than stiff materials, as discussed above.

B values calculated for the composites prepared with all the matrix polymers studied are collected in **Table 2**. It can be seen that parameter B covers a wide range from 1.5 to about 6, depending on the polymer in question. The second column of **Table 2** contains the calculated tensile strength of the composites, σ_0 (see **Eq. 1**). If these values is compared to parameter B it can be seen that they are not independent of each other; they express the principles mentioned above, i.e. reinforcement is stronger in weaker, soft matrices.

The model represented by **Eq. 1** was created using the assumption that in all

heterogeneous materials, including polymer composites, an interphase forms spontaneously which considerably influences properties. According to the model parameter B depends on the thickness (ℓ) and strength (σ_i) of the interphase and on the size of the interphase (A_f) in the following way

$$B = \left(1 + A_f \rho_f \ell\right) \ln \frac{\sigma_i}{\sigma_0}$$

(2)

where A_f is the specific surface area and ρ_f the density of the filler. According to **Eq. 2**, a linear correlation exists between parameter B and the natural logarithm of matrix strength.

Parameter B is plotted against matrix strength in **Fig. 5** and it can be seen that it corresponds to the prediction; a relatively close linear correlation is obtained with a negative slope for the ten polymers studied. The close relationship clearly proves that reinforcement depends on the characteristics of the matrix and cannot be judged from the composition dependence of tensile yield stress or strength. **Fig. 5** also proves that although parameter B depends also on interfacial interactions determining the thickness and properties of the interphase [26], it is dominated by matrix properties thus the effect of interactions is difficult or impossible to deduce from it. Deviations from the linear correlation indicate the effect of experimental error, but also that of interactions. In order to compensate for the effect of the matrix, a quantity taking into consideration matrix strength was calculated and listed in the last but one column of **Table 2**. It can be seen that the difference is much smaller in this quantity than either in parameter B or matrix strength, but it still does not help much to estimate matrix/filler interaction. Further approaches are needed for this purpose, some of which will be presented in the next sections.

3.3. Cyclic loading, debonding

If the interaction between the matrix and the filler results from secondary, van der Waals bonds, they are not very strong and under the effect of external load the matrix and the filler may separate at the interface, i.e. debonding occurs. Debonding stress depends

on the strength of interaction and can be estimated with the model developed by Vollenberg [27, 28] and Vörös [29], respectively. According to both models initiation stress depends on the strength of interfacial interaction, on the size of the particles and on the stiffness of the matrix [29], i.e.

$$\sigma^D = -C_1\sigma^T + C_2\sqrt{\frac{W_{AB}E}{R}}$$

(3)

where σ^D and σ^T are debonding and thermal stress, respectively, W_{AB} the reversible work of adhesion, E the Young's modulus of the matrix, R the radius of the particles, while C_1 and C_2 are constants. Accordingly, larger initiation stress is needed for debonding with increasing adhesion of the components, with increasing stiffness of the matrix and with decreasing particle size. Debonding experiments were carried out with increasing pre-strains as described in the experimental part and some results are presented in **Fig. 6**. Modulus decreases when debonding starts, thus debonding stress can be determined from the deviation of stiffness from the first, horizontal part of the correlation.

Debonding results in a three-component material consisting of the matrix, particles and voids. The amount of debonded zeolite can be estimated with the help of Hartingsveldt's approach [30]. The model assumes that bonded particles increase stiffness, while debonded particles do not. The dependence of composite modulus is expressed by the following expression [31]

$$E(\varphi) = \left(1 + \frac{\varphi_b}{\beta(1-\varphi_b)}\right)E_m$$

(4)

where E_m is the modulus of the matrix polymer, φ_b is the volume fraction of bonded particles and β is defined as

$$\beta = \frac{8 - 10\,v_m}{15(1 - v_m)}$$

(5)

where v_m is the Poisson's ratio of the matrix. Since debonded particles cannot carry any

load, modulus must be corrected by the effective load-bearing cross-section of the matrix, thus composite stiffness becomes

$$E_c = \left(1 - \varphi_d^{2/3}\right) E(\varphi_b)$$

(6)

and the amount of bonded particles is defined as

$$\varphi_b = \varphi_f - \varphi_d$$

(7)

where φ_f is total filler content, while φ_d is the volume fraction of debonded particles. If the modulus (E_c) of pre-strained composite samples is determined and v_m is known, the amount of bonded (φ_b) and debonded (φ_d) particles can be calculated from **Eqs. 4-7**. The amount of debonded particles is plotted against pre-strain in **Fig. 7** for the composites presented in the previous figure. It can be seen that debonding starts very early, at very small strains for PVC, while only at larger deformations for the two polyolefins presented in the figure, then proceeds almost to completion for all three of them. Practically all the particles are separated from the matrix yielding voids, if the strain is sufficiently large.

According to **Eq. 3**, debonding stress depends on the stiffness of the matrix and **Fig. 8** confirms this effect. Debonding stress determined from cyclic loading (σ^D_c) is plotted against the square root of matrix stiffness as suggested by **Eq. 3**. Although some of the points are grouped together, the correlation agrees well with the prediction of the model. Unfortunately, debonding stress could not be determined for all the matrices, since very stiff materials broke at very small deformations, before debonding started. Since σ^D_c is influenced also by thermal stresses, matrix stiffness and particle size, the determination of the strength of interaction is difficult, requires the knowledge of the parameters of **Eq. 3**.

3.4. Interactions

The results presented in the previous sections and the related discussion showed that interfacial interactions play a role in the determination of composite properties, but their estimation is not obvious in the present case. Various methods can be used for the estimation of the strength of interfacial adhesion. One approach used occasionally is the

11

determination of debonding stress from acoustic emission experiments [32], but could not be detected any signals during the tensile testing of the 1 mm thick specimens used in this study. Cyclic experiments could supply information for some of the composites, but debonding stress could not be determined for stiff and especially for brittle polymers.

Occasionally we try to draw conclusions about interfacial interactions from changes in parameter B. Parameter B is definitely influenced by the strength of interaction, which determines the thickness and properties of the interphase [26]. In the absence of structural effects like the orientation of anisotropic particles or aggregation, parameter B depends very much on interfacial adhesion and can be estimated from changes in B. In the present case, however, the strong influence of matrix properties on parameter B makes any estimate of the strength of interaction difficult. Nevertheless, based on the results it can be concluded that interfacial interactions are not very strong, since cyclic experiments yielded debonded particles and debonding strength could be determined by the method for some of the polymers. The strength of interaction differ for the polymers used shown by their dissimilar surface tension (see **Table 1**), but also by the deviation from the linear correlation in **Fig. 5**.

SEM is used quite frequently for the estimation of interfacial adhesion in polymer composites and the results obtained partially support our conclusions presented above. **Fig. 9** shows micrographs recorded on the fracture surface of selected composites. Debonding and considerable matrix yielding occurs in the LDPE composite (**Fig. 9a**), and clean debonding can be observed in the PP composite (**Fig. 9b**). The danger of using SEM for the estimation of interactions is demonstrated excellently by **Fig. 9c**, showing the micrograph taken from another PP composite at 50 vol% zeolite content. Particles are covered by the matrix thus one could easily draw the conclusion from the micrograph that interaction between the filler and the matrix is strong. However, the conclusion would be wrong and the micrograph is deceiving, since interactions cannot depend on composition, on the one hand, and all evidence (see **Fig. 6**) indicate weak interaction between PP and the zeolite, on the other. Finally the fracture surface of a SAN composite is shown in **Fig. 9d** showing again some debonding, although interpretation is not completely

unambiguous and up to opinion in this case as well. Apparently debonding initiated the failure of the composite at very small deformation that resulted also in the failure of the cyclic test for this polymer.

The usual and obvious route of using the reversible work of adhesion for the characterization of the strength of interaction could not be followed directly, because we encountered various problems during the determination of the surface tension of the zeolite. Because of its high surface energy, the apolar component of surface tension could be determined only at 280 °C by IGC and the polar component could not be measured even at this temperature because none of the polar solvents eluted from the column. On the other hand, this characteristic could be calculated from spreading pressure derived from the adsorption isotherm of water on the zeolite. Accordingly, 181.9 mJ/m^2 was obtained for the apolar (IGC) and 440.9 mJ/m^2 for the polar (adsorption) component of surface tension. Using these values in further calculations is somewhat questionable because they were determined at different temperatures. However, since the same zeolite was used in all composites, an approximate value is acceptable for comparative purposes. Accordingly, the reversible work of adhesion was calculated for all polymer/zeolite pairs and the results are listed in the last column of **Table 2**. It is obvious that interfacial adhesion is different in the composites, W_{AB} changes from around 200 to 280 mJ/m^2. The corrected parameter B (B ln σ_{T0}) used for the estimation of interactions above is plotted against the reversible work of adhesion in **Fig. 10**. A clear correlation exists between the two quantities proving that interfacial interactions influence composite properties and reinforcement indeed. On the other hand, the slope of the correlation is negative, although one would expect an increase in B with increasing interfacial adhesion. The apparent contradiction can be explained, and proves at the same time, that interactions are not very strong and composite properties, as well as reinforcement is determined mainly by matrix characteristics.

4. CONCLUSIONS

The study of the characteristics of polymer/zeolite desiccant composites prepared with ten different matrices showed that their properties change in a wide range. Stiffness varies between 0.3 and 10 GPa, while strength between l0 and 80 MPa. The deformability of most composites is small and decreases with increasing zeolite content. Interfacial adhesion between the matrix polymer and zeolite is not very strong although quantitative determination is hampered by various factors. Most of the composites fail by debonding thus debonding stress could be determined in cyclic loading and relaxation experiments. Brittle matrices fail by debonding and/or matrix fracture, while considerable shear yielding has been observed in LDPE composites. Composite properties are determined mainly by matrix characteristics and interfacial adhesion plays only a relatively minor role. Accordingly, the matrix of such desiccant composites must be selected mainly according to functional properties and always in view of matrix characteristics.

5. ACKNOWLEDGEMENTS

6. REFERENCES

[1] Realini CE, Marcos B. Active and intelligent packaging systems for a modern society. Meat Sci 2014;98(3):404-419.

[2] Wong EH, Rajoo R. Moisture absorption and diffusion characterisation of packaging materials—advanced treatment. Microelectron Reliab 2003;43(12):2087-2096.

[3] Allinson JG, Dansereau RJ, Sakr A. The effects of packaging on the stability of a

moisture sensitive compound. Int J Pharm 2001;221(1–2):49-56.

[4]   Waterman KC, MacDonald BC. Package selection for moisture protection for solid, oral drug products. J Pharm Sci 2010;99(11):4437-4452.

[5]   Naversnik K, Bohanec S. Predicting drug hydrolysis based on moisture uptake in various packaging designs. Eur J Pharm Sci 2008;35(5):447-456.

[6]   Mathiowitz E, Jacob JS, Jong YS, Hekal TM, Spano W, Guemonprez R, et al. Novel desiccants based on designed polymeric blends. J Appl Polym Sci 2001;80(3):317-327.

[7]   Pehlivan H, Özmıhçı F, Tıhmınlıoğlu F, Balköse D, Ülkü S. Water and water vapor sorption studies in polypropylene–zeolite composites. J Appl Polym Sci 2003;90(11):3069-3075.

[8]   Biswas J, Kim H, Choe S, Kundu P, Park Y-H, Lee D. Linear low density polyethylene (LLDPE)/zeolite microporous composite film. Macromol Res 2003;11(5):357-367.

[9]   Biswas J, Kim H, Shim SE, Kim GJ, Lee DS, Choe S. Comperative Study of zeolite filled LLDPE and HDPE composite films. J Ind Eng Chem 2004;10(4):582–591.

[10]   Kim H, Biswas J, Choe S. Effects of stearic acid coating on zeolite in LDPE, LLDPE, and HDPE composites. Polymer 2006;47(11):3981-3992.

[11]   Kim H, Biswas J, Choi HH, Kim GJ, Lee DS, Choe S. Preparation of a Novel Microporous HDPE/Zeolite Composite Film. J Ind Eng Chem 2003;9(6):655–665.

[12]   Özmihci F, Balköse D, Ülkü S. Natural zeolite polypropylene composite film preparation and characterization. J Appl Polym Sci 2001;82(12):2913-2921.

[13]   Rothon R. The high percormance fillers market and the position of precipitated calcium carbonate and silica. High Performance Fillers, Hamburg, Germany: Smithers Rapra Ltd.; 2007. p. 1-4.

[14]   Biswas J, Kim H, Choe S. Properties of highly filled polypropylene derivative composites containing calcite and zeolite. J Appl Polym Sci 2006;99(5):2627-2639.

[15]   Biswas J, Kim H, Yim C, Cho J, Kim G, Choe S, et al. Structural effects on the tensile and morphological properties of zeolite-filled polypropylene derivative composites.

Macromol Res 2004;12(5):443-450.

[16] Bledzki AK, Gassan J. Composites reinforced with cellulose based fibres. Prog Polym Sci 1999;24(2):221-274.

[17] Upadhyay RD, Kale DD. Effect of synthetic sodium aluminium silicate on the properties of nylon 6. Polym Int 2001;50(11):1209-1213.

[18] Metin D, Tihminlioglu F, Balköse D, Ülkü S. The effect of interfacial interactions on the mechanical properties of polypropylene/natural zeolite composites. Compos Part A 2004;35(1):23-32.

[19] Acosta JL, Morales E, Ojeda MC, Linares A. The effect of interfacial adhesion and morphology on the mechanical properties of polypropylene composites containing different acid surface treated sepiolites. J Mater Sci 1986;21(2):725-728.

[20] Yuzay IE, Auras R, Selke S. Poly(lactic acid) and zeolite composites prepared by melt processing: Morphological and physical–mechanical properties. J Appl Polym Sci 2010;115(4):2262-2270.

[21] Fekete E, Pukánszky B, Tóth A, Bertóti I. Surface Modification and Characterization of Particulate Mineral Fillers. J Colloid Interface Sci 1990;135(1):200-208.

[22] Kenyó C, Kajtár D, Renner K, Kröhnke C, Pukánszky B. Functional packaging materials: factors affecting the capacity and rate of water adsorption in desiccant composites. J Polym Res 2013;20(11):1-8.

[23] Turcsányi B, Pukánszky B, Tüdős F. Composition Dependence of Tensile Yield Stress in Filled Polymers. J Mater Sci Lett 1988;7(2):160-162.

[24] Pukánszky B. Influence of Interface Interaction on the Ultimate Tensile Properties of Polymer Composites. Composites 1990;21(3):255-262.

[25] Pukánszky B, Maurer FHJ. Composition Dependence of the Fracture-Toughness of Heterogeneous Polymer Systems. Polymer 1995;36(8):1617-1625.

[26] Vörös G, Fekete E, Pukánszky B. An interphase with changing properties and the mechanism of deformation in particulate-filled polymers. J Adhes 1997;64(1-4):229-250.

[27] Vollenberg P, Heikens D, Ladan HCB. Experimental-Determination of Thermal and Adhesion Stress in Particle Filled Thermoplasts. Polym Compos 1988;9(6):382-388.

[28] Vollenberg P. The mechanical behaviour of particle filled thermoplastics. Eindhoven University of Technology, Ph.D., 1987.

[29] Pukánszky B, Vörös G. Mechanism of interfacial interactions in particulate filled composites. Compos Interfaces 1993;1(5):411-427.

[30] van Hartingsveldt EAA, van Aartsen JJ. Interfacial Debonding in Polyamide-6 Glass Bead Composites. Polymer 1989;30(11):1984-1991.

[31] Chow TS. Effect of particle shape at finite concentration on the elastic moduli of filled polymers. J Polym Sci Part B 1978;16(6):959-965.

[32] Renner K, Yang MS, Móczó J, Choi HJ, Pukánszky B. Analysis of the debonding process in polypropylene model composites. Eur Polym J 2005;41(11):2520-2529.

7. CAPTIONS

Fig. 1   Young's modulus of selected polymer/desiccant composites plotted against zeolite content. Symbols: ($\triangle$) LDPE, ($\diamond$) PS, ($\bullet$) HIPS1, ($\star$) SAN.

Fig. 2   Effect of zeolite content on the tensile strength of composites prepared with various matrices. Symbols: ($\triangle$) LDPE, ($\diamond$) PS, ($\bullet$) HIPS1, ($\star$) SAN.

Fig. 3   Dependence of deformability on zeolite content in polymer/desiccant composites. Symbols: ($\triangle$) LDPE, ($\diamond$) PS, ($\bullet$) HIPS1, ($\star$) SAN.

Fig. 4   Reduced tensile strength of polymer/desiccant composites plotted against zeolite content according to **Eq. 1**. Determination of the extent of reinforcen ($\triangle$) LDPE, ($\star$) SAN.

Fig. 5   Linear correlation between the extent of reinforcement (parameter *B*) and matrix strength for polymer/zeolite composites.

Fig. 6   Cyclic loading test for the determination of debonding stress in polymer zeolite composites. Changes in modulus as a function of pre-strain. Symbols: ($\triangledown$) PVC, ($\circ$) PP, ($\square$) HDPE.

Fig. 7   Dependence of the amount of debonded particles on the pre-strain used in the cyclic loading experiment. Symbols: ($\triangledown$) PVC, ($\circ$) PP, ($\square$) HDPE.

Fig. 8   Correlation between debonding stress and matrix stiffness in polymer/zeolite composites.

Fig. 9   SEM micrographs recorded on the fracture surface of polymer/zeolite composites; a) LDPE, 50 vol%, b) PP, 20 vol%, c) PP, 50 vol%, d) SAN, 50 vol%.

Fig. 10   Correlation between quantities related to interfacial adhesion in polymer/zeolite composites.

Table 1 The most important characteristics of the polymers used in the experiments

Polymer	Source	MFI (g/10 min)		M_n (g/mol)	M_w/M_n	Density (g/cm^3)	Surface tension (mJ/m^2)		
		Value	Conditions				γ_S^d	γ_S^p	γ_S
LDPE	TVK, Hungary	0.28	190 °C, 2.16 kg	17160	6.89	0.92	32.5	0.3	32.8
HDPE	TVK, Hungary	0.35	190 °C, 2.16 kg	18620	6.57	0.96	33.2	0.6	33.8
PP	TVK, Hungary	2.50	230 °C, 2.16 kg	92620	4.84	0.90	32.0	0.8	33.0
PS	Dow, USA	2.50	200 °C, 5 kg	127970	2.44	1.04	40.8	1.6	42.4
HIPS1	Dow, USA	12.00	200 °C, 5 kg	77525	2.68	1.02	38.5	1.8	40.3
HIPS2	Dow, USA	2.80	200 °C, 5 kg	95840	2.54	1.04	38.1	1.6	39.7
SAN	Dow, USA	3.50	230 °C, 3.8 kg	75510	2.39	1.07	37.3	2.3	39.6
PC	Bayer, Germany	13.00	300 °C, 1.2 kg	24730	2.07	1.20	34.8	3.6	39.7
PMMA	Arkema, France	11.00	230 °C, 3.8 kg	43470	1.88	1.16	40.3	0.7	41.0
PVC	Borsodchem, Hungary	–	–	55270	2.41	1.44	34.7	4.2	38.7

Table 2　　Parameters characterizing reinforcement in polymer/zeolite composites calculated from their tensile strength

Polymer	σ_0[a] (MPa)	B	$R^{2(b)}$	$B\ln\sigma_0$	W_{AB} (mJ/m^2)
LDPE	13.5	6.08	0.9905	15.8	207.0
HDPE	30.2	5.09	0.9884	17.3	218.5
PP	39.6	4.72	0.9773	17.4	220.1
PS	38.3	1.80	0.9837	6.6	259.3
HIPS1	11.9	4.56	0.9926	11.3	256.6
HIPS2	14.3	3.91	0.9993	10.4	252.3
SAN	79.9	1.50	0.9951	6.6	260.8
PC	54.8	1.96	0.9519	7.8	270.1
PMMA	42.2	1.98	0.9582	7.4	240.0
PVC	34.7	1.73	0.9342	6.1	276.2

a) matrix strength calculated from the intersection of the linear correlations (see. Eq. 1)

b) determination coefficient indicating the accuracy of the fit

FIGURES

Figure 1.
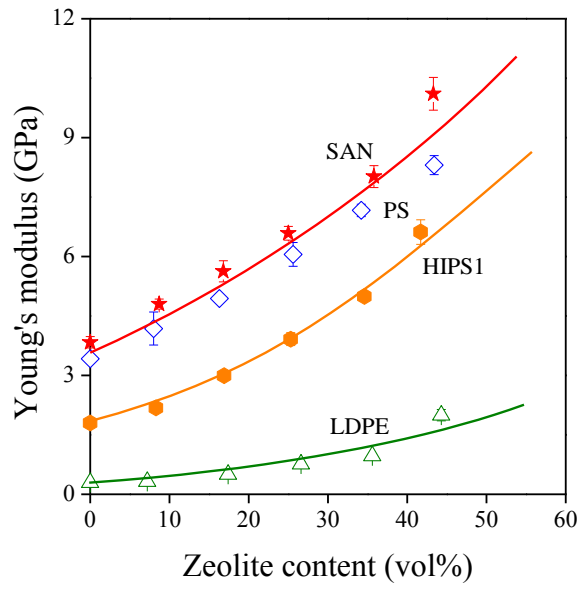
Figure 2.
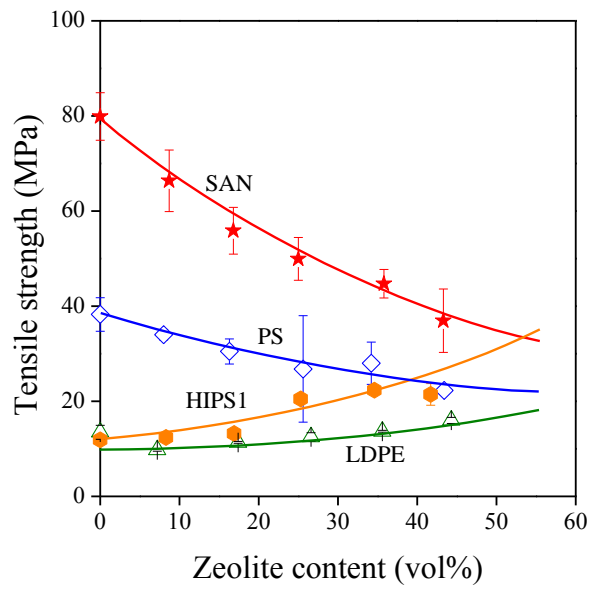
Figure 3.
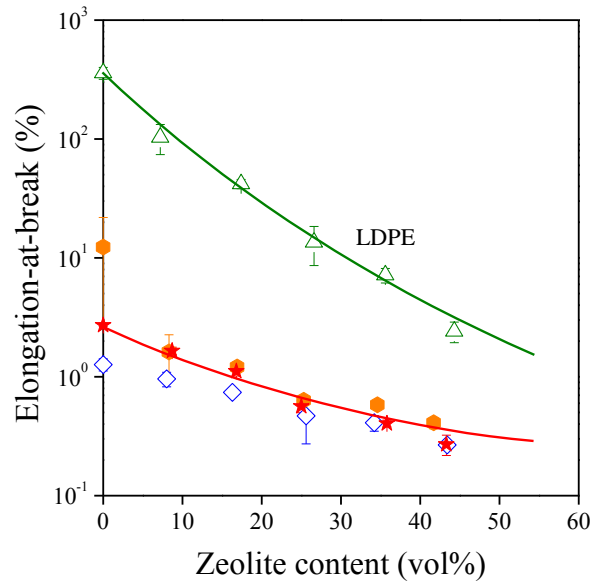
Figure 4.
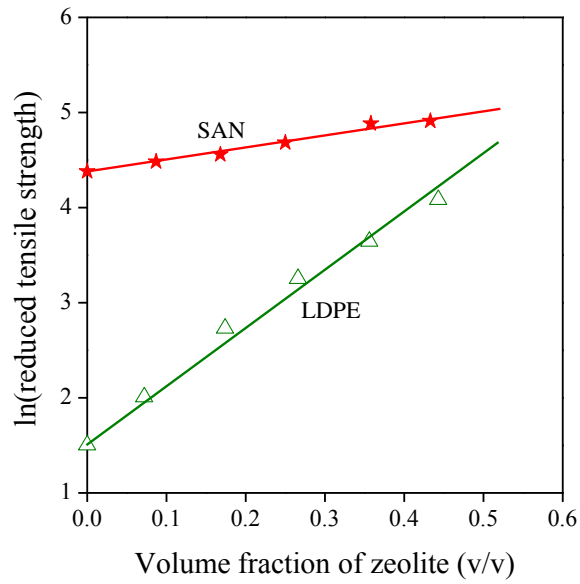
Figure 5.
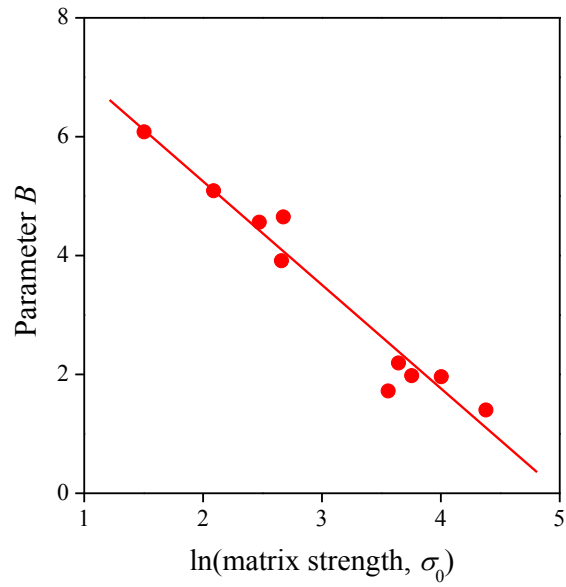
Figure 6.
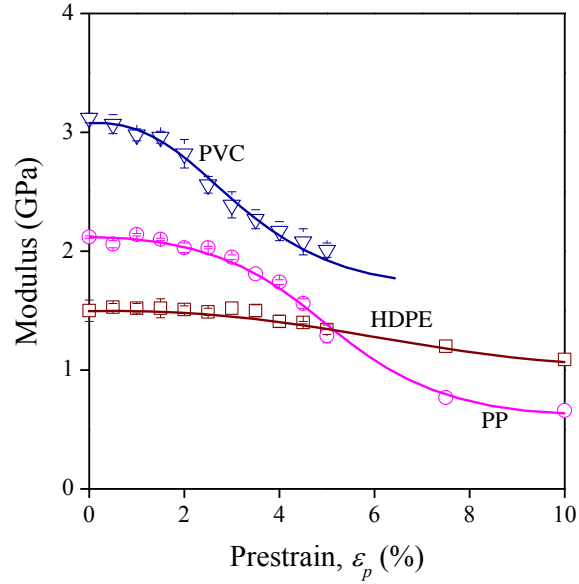
Figure 7.
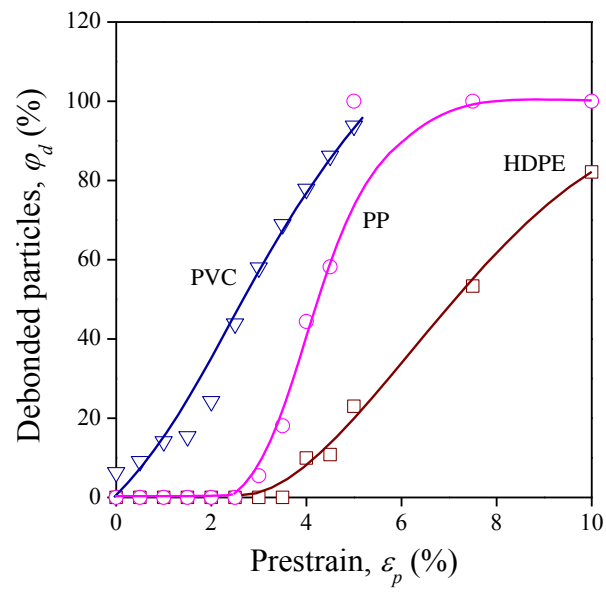
Figure 8

Figure 9.

Figure 10.